Blind Adaptive Beamformer Based on Orthogonal Projections for GNSS

Matteo Sgammini[(1)], Felix Antreich[(1)], Lothar Kurz [(2)] , Michael Meurer [(1)], and Tobias G. Noll [(2)]
(1) *German Aerospace Center (DLR), Germany*
(2) *RWTH Aachen University, Germany*

BIOGRAPHY

Matteo Sgammini received the BEng degree in electrical engineering in 2005 from the University of Perugia. He joined the Institute of Communications and Navigation of the German Aerospace Center (DLR) in 2008. His field of research is interference detection and mitigation for global navigation satellite systems (GNSS) .

Felix Antreich (IEEE M'06) received the diploma and the Ph.D. degree in Electrical Engineering and Information Technology from the Munich University of Technology (TUM), Munich, Germany, in 2003 and 2011, respectively. Since July 2003, he has been with the Institute of Communications and Navigation of the German Aerospace Center (DLR), Wessling-Oberpfaffenhofen, Germany. His research interests include sensor array signal processing for global navigation satellite systems (GNSS) and wireless communications, estimation theory and signal design for synchronization, and GNSS.

Michael Meurer received the diploma in Electrical Engineering and the Ph.D. degree from the University of Kaiserslautern, Germany. After graduation, he joined the Research Group for Radio Communications at the Technical University of Kaiserslautern, Germany, as a senior key researcher, where he was involved in various international and national projects in the field of communications and navigation both as project coordinator and as technical contributor. From 2003 till 2005, Dr. Meurer was active as a senior lecturer. Since 2005 he has been an Associate Professor (PD) at the same university. Additionally, since 2006 Dr. Meurer is with the German Aerospace Center (DLR), Institute for Communications and Navigation, where he is the director of the Department of Navigation.

Lothar Kurz received the Dipl.-Ing. degree in Electrical Engineering from RWTH Aachen University in 2007. Since then he is working as a PhD student at the Chair of Electrical Engineering and Computer Systems. His research interests are in the field of satellite navigation and processor design.

Tobias G. Noll received the Ing. (grad.) degree in Electrical Engineering from the Fachhochschule Koblenz, Germany in 1974, the Dipl-Ing. degree in Electrical Engineering from the Technical University of Munich in 1982, and the Dr.-Ing. degree from the Ruhr-University of Bochum in 1989. From 1974 to 1976, he was with the Max-Planck-Institute of Radio Astronomy, Bonn, Germany, being active in the development of microwave waveguide and antenna components. Since 1976 he was with the Corporate Research and Development Department of Siemens and since 1987 he headed a group of laboratories concerned with the design of algorithm specific integrated CMOS circuits for high-throughput digital signal processing. In 1992, he joined the Electrical Engineering Faculty of the RWTH Aachen University, Germany, where he is a Professor, holding the Chair of Electrical Engineering and Computer Systems. In addition to teaching, he is involved in research activities on VLSI architectural strategies for high-throughput digital signal processing, circuits concepts, and design methodologies with a focus on low power CMOS and deep submicron issues, as well as on digital signal processing for medicine electronics.

INTRODUCTION

The quality of the ranging data provided by a global navigation satellite systems (GNSS) receiver largely depends on the synchronization error, that is, on the accuracy of the propagation time-delay estimation of the line-of-sight (LOS) signal. In case the LOS signal is corrupted by several superimposed delayed replicas (reflective, diffractive, or refractive multipath) and/or additional radio frequency

interference (RFI), the estimation of the propagation time-delay and thus the position can be severely degraded using state-of-the-art GNSS receivers. Multi-antenna GNSS receivers enable application of array processing for effective multipath and interference mitigation. Especially, beamforming (spatial filtering) approaches have been studied intensely for GNSS in the past years due to a balanced trade-off between performance and complexity, e.g. as presented in [1, 2, 3, 4, 5]. Usually beamforming approaches require knowledge of the spatial signature (spatial reference) of the desired signal and thus require detailed knowledge of the direction-of-arrival (DoA) of the LOS signal and/or non-LOS (NLOS) signals, the antenna response, the array geometry, and other hardware biases. Even if the antenna array response can be approximately determined, either by empirical measurements (array calibration) or by making certain assumptions (e.g. identical sensor elements in known locations), the true antenna array response can be significantly different due to for example changes in antenna location, temperature, calibration inaccuracy and the surrounding environment [6, 7, 8]. Thus, robust beamforming algorithms have to be developed in order to cope with errors in the array response model to be applied and to be tailored to GNSS to derive the respective spatial filter [4, 9].

In this work we propose a two-step blind adaptive beamforming approach based on orthogonal projections for GNSS, for which knowledge of the array response and a spatial reference for the LOS signal are not required. The proposed approach is capable of adaptively mitigating RFI and multipath components based on orthogonal projections. In order to derive the needed projectors adaptively two eigendecompositions of an estimate of the spatial covariance matrix before (pre-correlation) and after (post-correlation) despreading are performed. Based on these eigendecompositions we apply a projector onto the interference free subspace at pre-correlation stage and a blind adaptive eigenbeamformer in order to maximize the ratio between the power of the desired LOS and the power of the undesired NLOS signals plus noise at post-correlation stage.

Two different approaches tailored to the different needs are presented in order to derive these eigendecompositions. A cost-analysis in terms of processing cycles on an embedded processor for the covariance matrix computation and eigendecomposition is provided.

A software bit accurate representation of the GNSS receiver hardware platform is used for performance evaluation. Simulation results show that the proposed blind adaptive beamforming approach based on orthogonal projections is capable of effectively mitigating interference and multipath signals. As the proposed blind approach does not require *a priori* information about the DoAs of the LOS or NLOS signals and about the antenna array response, robustness with respect to errors in the antenna array response model and additional hardware biases can be achieved without further increase of complexity.

SIGNAL MODEL

The complex baseband signal with bandwidth B that is received by an antenna array with M sensor elements is

$$\mathbf{x}(t) = \mathbf{s}(t) + \mathbf{z}(t) + \mathbf{n}(t) = \sum_{\ell=1}^{L} \mathbf{s}_\ell(t) + \sum_{i=1}^{I} \mathbf{z}_i(t) + \mathbf{n}(t), \tag{1}$$

where $\mathbf{s}(t)$ $\mathbb{C}^{M\times 1}$ denotes the superimposed signal replicas

$$\mathbf{s}_\ell(t) = \mathbf{a}\left(\phi_\ell, \vartheta_\ell\right)\ \gamma_\ell\ \mathrm{e}^{\mathrm{j}2\pi\nu_\ell t} c(t-\tau_\ell), \tag{2}$$

$\mathbf{a}\left(\phi_\ell, \vartheta_\ell\right) \in \mathbb{C}^{M\times 1}$ defines the steering vector of an antenna array with azimuth angle ϕ_ℓ and elevation angle ϑ_ℓ, $c(t-\tau_\ell)$ denotes a periodically repeated pseudo random (PR) sequence $c(t)$ with time-delay τ_ℓ, chip duration T_c, and period $T = N_c T_c$ with $N_c \in \mathbb{N}$. γ_ℓ is the complex amplitude, ν_ℓ is the Doppler frequency, and $\mathbf{z}(t)$ $\mathbb{C}^{M\times 1}$ denotes superimposed radio interference signals where

$$\mathbf{z}_i(t) = \mathbf{a}\left(\phi_i, \vartheta_i\right)\ b_i(t), \tag{3}$$

and $b_i(t)$ defines the i-th radio interference signal with $i = 1, \ldots, I$. Additionally, we assume temporally and spatially white complex Gaussian noise $\mathbf{n}(t) \in \mathbb{C}^{M\times 1}$. In the following the parameters of the LOS signal are indicated with $\ell = 1$ and the parameters of the NLOS signals (multipath) with $\ell = 2, \ldots, L$.

The spatial observations are collected at K periods of the PR sequence at N time instances, thus $\mathbf{x}[(k-1)N+n] = \mathbf{x}(((k-1)N+n)\,T_s)$ with $n = 1, \ldots, N$, $k = 1, \ldots, K$, and the sampling frequency $\frac{1}{T_s} \geq 2B$. The channel parameters are assumed constant during the k-th period of the observation interval. Collecting the samples of the k-th period of the observation interval we define the $M \times N$ complex matrices:

$$\mathbf{X}[k] = \left[\mathbf{x}[(k-1)N+1], \ldots, \mathbf{x}[(k-1)N+n], \ldots, \mathbf{x}[(k-1)N+N]\right], \tag{4}$$

$$\mathbf{N}[k] = \left[\mathbf{n}[(k-1)N+1], \ldots, \mathbf{n}[(k-1)N+n], \ldots, \mathbf{n}[(k-1)N+N]\right], \tag{5}$$

$$\mathbf{S}[k] = \left[\mathbf{s}[(k-1)N+1], \ldots, \mathbf{s}[(k-1)N+n], \ldots, \mathbf{s}[(k-1)N+N]\right], \tag{6}$$

$$\mathbf{Z}[k] = \left[\mathbf{z}[(k-1)N+1], \ldots, \mathbf{z}[(k-1)N+n], \ldots, \mathbf{z}[(k-1)N+N]\right]. \tag{7}$$

Thus, the signal can be written in matrix notation as

$$\begin{aligned} \mathbf{X}[k] &= \mathbf{S}[k] + \mathbf{Z}[k] + \mathbf{N}[k] \\ &= \mathbf{A}_s[k]\mathbf{\Gamma}[k]\left(\mathbf{C}[k] \odot \mathbf{D}[k]\right) \\ &\quad + \mathbf{A}_z[k]\mathbf{B}[k] + \mathbf{N}[k], \end{aligned} \tag{8}$$

where $\odot$ denotes the Hadamard-Schur product,

$$\mathbf{A}_s[k] = [\mathbf{a}(\phi_1, \vartheta_1), \ldots, \mathbf{a}(\phi_\ell, \vartheta_\ell), \ldots, \mathbf{a}(\phi_L, \vartheta_L)] \in \mathbb{C}^{M\times L} \tag{9}$$

and

$$\mathbf{A}_z[k] = [\mathbf{a}(\phi_1, \vartheta_1), \ldots, \mathbf{a}(\phi_i, \vartheta_i), \ldots, \mathbf{a}(\phi_I, \vartheta_I)] \in \mathbb{C}^{M\times I} \tag{10}$$

denote the steering matrices,

$$\mathbf{\Gamma}[k] = \mathrm{diag}\{\boldsymbol{\gamma}\} \in \mathbb{C}^{L\times L} \quad (11)$$

is a diagonal matrix whose entries are complex amplitudes of the signal replicas $\boldsymbol{\gamma} = [\gamma_1, \ldots, \gamma_L]^{\mathrm{T}}$. Furthermore,

$$\mathbf{C}[k] = [\mathbf{c}[k;\tau_1]\cdots\mathbf{c}[k;\tau_\ell]\cdots\mathbf{c}[k;\tau_L]]^{\mathrm{T}} \in \mathbb{R}^{L\times N} \quad (12)$$

contains the sampled and shifted $c(t)$ for each impinging wavefront

$$\mathbf{c}[k;\tau_\ell]=[c(((k-1)N+1)T_s-\tau_\ell),\ldots,c(((k-1)N+n)T_s-\tau_\ell), \ldots,c(((k-1)N+N)T_s-\tau_\ell)]^{\mathrm{T}}, \quad (13)$$

$$\mathbf{D}[k] = [\mathbf{d}[k;\nu_1]\cdots\mathbf{d}[k;\nu_\ell]\cdots\mathbf{d}[k;\nu_L]]^{\mathrm{T}} \in \mathbb{C}^{L\times N} \quad (14)$$

contains the complex exponential functions conveying the Doppler frequency of each wavefront

$$\mathbf{d}[k;\nu_\ell]=\left[\mathrm{e}^{\mathrm{j}2\pi\nu_\ell((k-1)N+1)T_s},\ldots,\mathrm{e}^{\mathrm{j}2\pi\nu_\ell((k-1)N+n)T_s}, \ldots,\mathrm{e}^{\mathrm{j}2\pi\nu_\ell((k-1)N+N)T_s}\right]^{\mathrm{T}}, \quad (15)$$

and

$$\mathbf{B}[k] = [\mathbf{b}_1[k]\cdots\mathbf{b}_i[k]\cdots\mathbf{b}_I[k]]^{\mathrm{T}} \in \mathbb{C}^{I\times N} \quad (16)$$

contains the sampled $b_i(t)$ for each interference signal

$$\mathbf{b}_i[k]=[b_i(((k-1)N+1)T_s),\ldots,b_i(((k-1)N+n)T_s),\ldots, b_i(((k-1)N+N)T_s)]^{\mathrm{T}}. \quad (17)$$

In general $||\mathbf{c}[k;\tau_\ell]||_2^2 \neq N, \forall\tau_\ell\ \forall_k$, but for the problem at hand[1] we can assume that $||\mathbf{c}[k;\tau_\ell]||_2^2 \approx N, \forall\tau_\ell\ \forall k$.
The spatial covariance matrix of the received signal considering the k-th period can be given as

$$\mathbf{R}_{\mathbf{xx}}[k] = \mathrm{E}\left[\mathbf{x}[(k-1)N+n]\mathbf{x}^{\mathrm{H}}[(k-1)N+n]\right]. \quad (18)$$

Assuming $\mathrm{E}\left[\mathbf{s}[(k-1)N+n]\mathbf{z}^{\mathrm{H}}[(k-1)N+n]\right] = \mathbf{0}$, $\mathrm{E}\left[\mathbf{s}[(k-1)N+n]\mathbf{n}^{\mathrm{H}}[(k-1)N+n]\right] = \mathbf{0}$, and $\mathrm{E}\left[\mathbf{n}[(k-1)N+n]\mathbf{z}^{\mathrm{H}}[(k-1)N+n]\right] = \mathbf{0}$ we get

$$\mathbf{R}_{\mathbf{xx}}[k] = \mathbf{R}_{\mathbf{ss}}[k] + \mathbf{R}_{\mathbf{zz}}[k] + \mathbf{R}_{\mathbf{nn}}[k], \quad (19)$$

with

$$\mathbf{R}_{\mathbf{ss}}[k] = \mathbf{A}_s[k]\mathbf{R}_{\mathbf{s's'}}[k]\mathbf{A}_s^{\mathrm{H}}[k], \quad (20)$$
$$\mathbf{R}_{\mathbf{zz}}[k] = \mathbf{A}_z[k]\mathbf{R}_{\mathbf{z'z'}}[k]\mathbf{A}_z^{\mathrm{H}}[k], \quad (21)$$
$$\mathbf{R}_{\mathbf{nn}}[k] = \sigma_n^2\mathbf{I}_M. \quad (22)$$

Here, $\mathbf{R}_{\mathbf{s's'}}[k] \in \mathbb{C}^{L\times L}$ and $\mathbf{R}_{\mathbf{z'z'}}[k] \in \mathbb{C}^{I\times I}$ denote the signal and interference covariance matrix, respectively.

[1] e.g. in case of GPS C/A PR sequences with bandwidth $B \geq 1.023$ MHz

PREWHITENING AND EIGENBEAMFORMING

In this section we will derive a two-step blind beamforming approach based on orthogonal projections. This approach consists of a pre-correlation prewhitening to spatially suppress radio interference signals and of a post-correlation blind eigenbeamforming in order to maximize the ratio between the power of the desired LOS signal and the power of the undesired NLOS signals plus noise.

Prewhitening

As the power of the signal replicas $\mathbf{s}_\ell(t)$ is much smaller than the power of the noise and the interference (in general about -20 to -40 dB) the spatial covariance matrix $\mathbf{R}_{\mathbf{xx}}[k]$ can be approximated by

$$\begin{aligned}\mathbf{R}_{\mathbf{xx}}[k] &\approx \mathbf{R}_{\mathbf{zz}}[k] + \mathbf{R}_{\mathbf{nn}}[k] \\ &= \mathbf{A}_z[k]\mathbf{R}_{\mathbf{z'z'}}[k]\mathbf{A}_z^{\mathrm{H}}[k] + \sigma_n^2\mathbf{I}_M. \end{aligned} \quad (23)$$

Thus, an eigendecomposition of $\mathbf{R}_{\mathbf{xx}}[k]$ can be expressed as

$$\mathbf{R}_{\mathbf{xx}}[k] \approx [\mathbf{U}_I\mathbf{U}_N]\left(\begin{bmatrix}\mathbf{\Lambda}_I & \mathbf{0}\\ \mathbf{0} & \mathbf{0}\end{bmatrix} + \sigma_n^2\mathbf{I}_M\right)\begin{bmatrix}\mathbf{U}_I^{\mathrm{H}}\\ \mathbf{U}_N^{\mathrm{H}}\end{bmatrix}, \quad (24)$$

where the columns of the unitary matrix $\mathbf{U}_I \in \mathbb{C}^{M\times I}$ span the interference subspace, the columns of the unitary matrix $\mathbf{U}_N \in \mathbb{C}^{M\times(M-I)}$ span the noise subspace, and $\mathbf{\Lambda}_I$ denotes a diagonal matrix which contains the non-zero eigenvalues $\lambda_1, \ldots, \lambda_i, \ldots, \lambda_I$ with respect to the interference subspace in the noise free case. A prewhitening matrix to prewhiten $\mathbf{X}[k]$ can be given by

$$\mathbf{R}_{\mathbf{xx}}^{-\frac{1}{2}}[k] \approx \mathbf{U}_I\left(\mathbf{\Lambda}_I + \sigma_n^2\mathbf{I}_I\right)^{-\frac{1}{2}}\mathbf{U}_I^{\mathrm{H}} + \frac{1}{\sqrt{\sigma_n^2}}\mathbf{U}_N\mathbf{U}_N^{\mathrm{H}}. \quad (25)$$

For $\lambda_i >> \sigma_n^2$, i.e. in case of strong interference, we get

$$\mathbf{R}_{\mathbf{xx}}^{-\frac{1}{2}}[k] \approx \frac{1}{\sqrt{\sigma_n^2}}\mathbf{U}_N\mathbf{U}_N^{\mathrm{H}} = \frac{1}{\sqrt{\sigma_n^2}}\mathbf{P}_I^{\perp}[k], \quad (26)$$

where $\mathbf{P}_I^{\perp}[k]$ is the projector onto the interference free subspace for the k-th period.
Now, we can apply the projector $\mathbf{P}_I^{\perp}[k]$ in order to prewhiten $\mathbf{X}[k]$ and thus to suppress the interference

$$\begin{aligned}\tilde{\mathbf{X}}[k] &= \mathbf{P}_I^{\perp}[k]\mathbf{X}[k] \\ &= \mathbf{P}_I^{\perp}[k]\mathbf{A}_s[k]\ \mathbf{\Gamma}[k]\ (\mathbf{C}[k]\odot\mathbf{D}[k]) \\ &+ \underbrace{\mathbf{P}_I^{\perp}[k]\mathbf{A}_z[k]\ \mathbf{B}[k] + \mathbf{P}_I^{\perp}[k]\mathbf{N}[k]}_{=\tilde{\mathbf{N}}[k]}. \end{aligned} \quad (27)$$

The covariance of the prewhitened received signal $\tilde{\mathbf{X}}[k]$ can be given as

$$\mathbf{R}_{\tilde{\mathbf{x}}\tilde{\mathbf{x}}}[k] = \mathbf{P}_I^{\perp}[k]\mathbf{R}_{\mathbf{ss}}[k]\mathbf{P}_I^{\perp}[k] + \mathbf{R}_{\tilde{\mathbf{n}}\tilde{\mathbf{n}}}, \quad (28)$$

$$\tilde{\mathbf{X}}[k]=\left[\tilde{\mathbf{x}}[(k-1)N+1],\ldots,\tilde{\mathbf{x}}[(k-1)N+n],\ldots,\tilde{\mathbf{x}}[(k-1)N+N]\right], \quad (29)$$

$$\tilde{\mathbf{N}}[k]=\left[\tilde{\mathbf{n}}[(k-1)N+1],\ldots,\tilde{\mathbf{n}}[(k-1)N+n],\ldots,\tilde{\mathbf{n}}[(k-1)N+N]\right]. \quad (30)$$

Assuming (26) holds, we get

$$\mathbf{R}_{\tilde{\mathbf{x}}\tilde{\mathbf{x}}}[k] \approx \mathbf{P}_I^{\perp}[k]\mathbf{R}_{\mathbf{ss}}[k]\mathbf{P}_I^{\perp}[k] + \sigma_n^2\mathbf{I}_M. \quad (31)$$

The projector $\mathbf{P}_I^{\perp}[k]$ can be derived from an eigendecomposition of an estimate of the pre-correlation spatial covariance matrix of the k-th period $\hat{\mathbf{R}}_{\mathbf{xx}}[k]$. An estimate of the spatial covariance matrix can be achieved with a recursive implementation

$$\hat{\mathbf{R}}_{\mathbf{xx}}[(k-1)N+n] = \mu_{\mathbf{x}}\,\hat{\mathbf{R}}_{\mathbf{xx}}[(k-1)N+n-1] + (1-\mu_{\mathbf{x}})\,\mathbf{x}[(k-1)N+n]\mathbf{x}^{\mathrm{H}}[(k-1)N+n] \quad (32)$$

where $\mu_{\mathbf{x}}$ is the *"forgetting factor"* (or *"fading factor"*) with

$$\mu_{\mathbf{x}} = 1 - \frac{T_s}{T_{\mathbf{x}}}, \quad 0 \leq \mu_{\mathbf{x}} \leq 1 \quad (33)$$

where $T_{\mathbf{x}}$ is the desired covariance matrix observation time and $T_{\mathbf{x}} \geq T_s$.

Eigenbeamforming

Using an estimate of the LOS signal parameters τ_1 and ν_1 the signal after despreading (post-correlation) can be given as

$$\mathbf{y}[k] = \tilde{\mathbf{X}}[k]\frac{1}{N}(\mathbf{c}[k;\hat{\tau}_1] \odot \mathbf{d}[k;\hat{\nu}_1])^* \in \mathbb{C}^{M\times 1}, \quad (34)$$

where we define the post-correlation data matrix

$$\mathbf{Y} = [\mathbf{y}[1],\ldots,\mathbf{y}[k],\ldots,\mathbf{y}[K]] \in \mathbb{C}^{M\times K}. \quad (35)$$

Furthermore, we define

$$\bar{\mathbf{s}}[k]=\mathbf{P}_I^{\perp}[k]\mathbf{A}_s[k]\mathbf{\Gamma}[k](\mathbf{C}[k]\odot\mathbf{D}[k])\,\tfrac{1}{N}(\mathbf{c}[k;\hat{\tau}_1]\odot\mathbf{d}[k;\hat{\nu}_1])^* = \mathbf{P}_I^{\perp}[k]\mathbf{A}_s[k]\mathbf{\Gamma}[k]\begin{bmatrix}\delta_1[k]\\ \vdots \\ \delta_L[k]\end{bmatrix} = \mathbf{P}_I^{\perp}[k]\mathbf{A}_s[k]\mathbf{\Gamma}[k]\boldsymbol{\delta}[k], \quad (36)$$

$$\bar{\mathbf{n}}[k] = \tilde{\mathbf{N}}[k]\frac{1}{N}(\mathbf{c}[k;\hat{\tau}_1] \odot \mathbf{d}[k;\hat{\nu}_1])^* \in \mathbb{C}^{M\times 1}, \quad (37)$$

$$\bar{\mathbf{S}} = [\bar{\mathbf{s}}[1],\ldots,\bar{\mathbf{s}}[k],\ldots,\bar{\mathbf{s}}[K]] \in \mathbb{C}^{M\times K}, \quad (38)$$

$$\bar{\mathbf{N}} = [\bar{\mathbf{n}}[1],\ldots,\bar{\mathbf{n}}[k],\ldots,\bar{\mathbf{n}}[K]] \in \mathbb{C}^{M\times K}. \quad (39)$$

The post-correlation signal can be defined as

$$\mathbf{Y} = \bar{\mathbf{S}} + \bar{\mathbf{N}}, \quad (40)$$

and the post-correlation spatial covariance matrix can be given as

$$\mathbf{R}_{\mathbf{yy}} = \mathrm{E}\left[\mathbf{y}[k]\mathbf{y}^{\mathrm{H}}[k]\right]. \quad (41)$$

With $\mathrm{E}\left[\bar{\mathbf{s}}[k]\bar{\mathbf{n}}^{\mathrm{H}}[k]\right] = \mathbf{0}$ we get

$$\mathbf{R}_{\mathbf{yy}} = \mathbf{R}_{\bar{\mathbf{s}}\bar{\mathbf{s}}} + \mathbf{R}_{\bar{\mathbf{n}}\bar{\mathbf{n}}}, \quad (42)$$

with

$$\mathbf{R}_{\bar{\mathbf{s}}\bar{\mathbf{s}}} = \mathrm{E}\left[\bar{\mathbf{s}}[k]\bar{\mathbf{s}}^{\mathrm{H}}[k]\right], \quad (43)$$

$$\mathbf{R}_{\bar{\mathbf{n}}\bar{\mathbf{n}}} = \mathrm{E}\left[\bar{\mathbf{n}}[k]\bar{\mathbf{n}}^{\mathrm{H}}[k]\right] = \frac{\sigma_n^2}{N}\mathbf{I}_M. \quad (44)$$

Here, $10\log_{10}(N)$ denotes the despreading gain.
Now, let us derive the post-correlation eigenbeamformer. In general one can write

$$r[k] = \mathbf{w}^{\mathrm{H}}\mathbf{y}[k], \quad (45)$$

where $\mathbf{w} \in \mathbb{C}^{M\times 1}$ is the weight vector or beamforming vector and $r[k]$ is the scalar output of the beamformer. Using an eigendecomposition of the post-correlation signal covariance matrix $\mathbf{R}_{\bar{\mathbf{s}}\bar{\mathbf{s}}}$ we can write

$$\mathbf{R}_{\mathbf{yy}} = \lambda_d\mathbf{u}_d\mathbf{u}_d^{\mathrm{H}} + \mathbf{U}\mathbf{\Lambda}\mathbf{U}^{\mathrm{H}} + \frac{\sigma_n^2}{N}\mathbf{I}_M, \quad (46)$$

where λ_d denotes the dominant non-zero eigenvalue of the post-correlation signal covariance matrix $\mathbf{R}_{\bar{\mathbf{s}}\bar{\mathbf{s}}}$, $\mathbf{u}_d$ denotes the eigenvector with respect to λ_d, $\mathbf{\Lambda}$ is a diagonal matrix collecting the remaining non-zero eigenvalues $\lambda_2,\ldots,\lambda_\ell,\ldots,\lambda_L$ of $\mathbf{R}_{\bar{\mathbf{s}}\bar{\mathbf{s}}}$ besides λ_d, the unitary matrix $\mathbf{U} \in \mathbb{C}^{M\times(L-1)}$ collects the eigenvector with respect to the eigenvalues $\lambda_2,\ldots,\lambda_\ell,\ldots,\lambda_L$. If the LOS signal and the NLOS signals are not highly correlated, the dominant eigenvector $\mathbf{u}_d$ spans the LOS signal subspace and $\mathbf{U}$ spans the NLOS signal subspace. If the signals are highly correlated or even coherent appropriate preprocessing steps like forward-backward averaging [10] and spatial smoothing [11] can be applied to decorrelate the LOS and the NLOS signals.
Thus, we can formulate the optimization problem to derive a beamformer which maximizes the ratio between the power of the desired and the power of the undesired signals plus noise

$$\max_{\mathbf{w}} \frac{\mathbf{w}^{\mathrm{H}}\lambda_d\mathbf{u}_d\mathbf{u}_d^{\mathrm{H}}\mathbf{w}}{\mathbf{w}^{\mathrm{H}}\left(\mathbf{U}\mathbf{\Lambda}\mathbf{U}^{\mathrm{H}} + \frac{\sigma_n^2}{N}\mathbf{I}_M\right)\mathbf{w}}, \quad (47)$$

This results to an eigenvalue problem with the optimum weight vector

$$\mathbf{w}_{opt} = \mathbf{u}_d. \quad (48)$$

This beamformer we call eigenbeamformer.
The optimum beamforming weight $\mathbf{w}_{opt}$ can be derived from the eigenvector with respect to the dominant eigenvalue of the eigendecomposition of an estimate of the post-correlation spatial covariance matrix $\hat{\mathbf{R}}_{\mathbf{yy}}$. Following (32), we can derive an estimate of the spatial covariance matrix with a recursive implementation

$$\hat{\mathbf{R}}_{\mathbf{yy}}[k] = \mu_{\mathbf{y}}\,\hat{\mathbf{R}}_{\mathbf{yy}}[k-1] + (1-\mu_{\mathbf{y}})\,\mathbf{y}[k]\mathbf{y}^{\mathrm{H}}[k] \quad (49)$$

with

$$\mu_{\mathbf{y}} = 1 - \frac{T}{T_{\mathbf{y}}}\,, \quad 0 \leq \mu_{\mathbf{y}} \leq 1 \tag{50}$$

where $T_{\mathbf{y}}$ is the desired covariance matrix observation time and $T_{\mathbf{y}} \geq T$.

EIGENDECOMPOSITION

The prewhitening at pre-correlation stage and the eigenbeamforming at post-correlation stage have been defined in previous sections. In order to demonstrate the feasibility on embedded GNSS receivers, a cost-analysis in terms of hardware requirements is provided in this section.
Concerning the prewhitening, the number of eigenvalue/-vector pairs required for computing the projector $\mathbf{P}_I^{\perp}[k]$ is related to the number of interferers I. Thus, a complete decomposition of the spatial covariance matrix $\mathbf{R}_{\mathbf{xx}}[k]$ as defined in (24) has to be computed. Following (48), only the eigenvector $\mathbf{u}_d$ referring to the dominant eigenvalue λ_d of $\mathbf{R}_{\mathbf{yy}}$ is required for the eigenbeamforming at post-correlation stage. This matter of fact allows for choosing a simpler approach in terms of computational requirements for the latter case. In the following, two different algorithms for the eigendecomposition are presented that have been chosen with respect to an efficient implementation on an embedded receiver platform.

Jacobi algorithm

The Jacobi method is widely known as a robust choice in terms of numerical stability and it is an efficient algorithm for the decomposition of matrices of moderate order [12]. Thus, it has been chosen for the decomposition of $\hat{\mathbf{R}}_{\mathbf{xx}}[k]$. The Jacobi algorithm is briefly summarized in Alg.1 in order to provide an overview on several implementation details that have been considered for the cost-analysis on an embedded receiver platform. The basic strategy is to turn a matrix $\mathbf{R}_0 \in \mathbb{C}^{M\times M}$ into a diagonal matrix $\mathbf{R}_P = \mathrm{diag}\{\lambda_1, \ldots, \lambda_m, ..., \lambda_M\}$ with $m = 1, 2, \ldots, M$ by means of P similarity transforms, while $\lambda_1, \ldots, \lambda_m, \ldots, \lambda_M$ represent an approximation of the eigenvalues of $\hat{\mathbf{R}}_{\mathbf{xx}}[k]$ after P iterations. The eigenvector referring to λ_m can be obtained from the respective m-th column of $\mathbf{U}_P$.

Algorithm 1 Jacobi decomposition

1: $\mathbf{R}_0 = \hat{\mathbf{R}}_{\mathbf{xx}}[k], \mathbf{U}_0 = \mathbf{I}_M$
2: **for** $p = 0 \rightarrow P-1$ **do**
3: $\quad \mathbf{R}_{p+1} = \mathbf{G}_p^H \cdot \mathbf{R}_p \cdot \mathbf{G}_p$
4: $\quad \mathbf{U}_{p+1} = \mathbf{U}_p \cdot \mathbf{G}_p$
5: **end for**

Similarity transformations are implemented using Givens rotations as defined by the matrix $\mathbf{G}_p$ which is an identity matrix except for matrix elements in the m-th and m'-th columns and rows with $m' = m+1, \ldots, M$:

$$\mathbf{G}_p = \begin{bmatrix} 1 & \cdots & 0 & \cdots & 0 & \cdots & 0 \\ \vdots & \ddots & \vdots & & \vdots & & \vdots \\ 0 & \cdots & g_{m,m} & \cdots & g_{m,m'} & \cdots & 0 \\ \vdots & & \vdots & \ddots & \vdots & & \vdots \\ 0 & \cdots & g_{m',m} & \cdots & g_{m',m'} & \cdots & 0 \\ \vdots & & \vdots & & \vdots & \ddots & \vdots \\ 0 & \cdots & 0 & \cdots & 0 & \cdots & 1 \end{bmatrix} \tag{51}$$

with

$$g_{m,m} = \cos\phi, \tag{52}$$
$$g_{m,m'} = \sin\phi, \tag{53}$$
$$g_{m',m} = \mathrm{e}^{-\mathrm{j}\alpha}\sin\phi, \tag{54}$$
$$g_{m',m'} = \mathrm{e}^{-\mathrm{j}\alpha}\cos\phi, \tag{55}$$
$$\alpha = \arctan\left(\Im\{r_{m,m'}\}, \Re\{r_{m,m'}\}\right), \tag{56}$$
$$\phi = \frac{1}{2}\arctan\frac{2\cdot\Re\{r_{m,m'}\cdot\mathrm{e}^{-\mathrm{j}\alpha}\}}{\Re\{r_{m',m'} - r_{m,m}\}}. \tag{57}$$

$r_{m,m'}$, $r_{m',m'}$, and $r_{m,m}$ denote matrix elements of $\mathbf{R}_p$ and m and m' are determined by successively choosing a pivot element $r_{m,m'}$ from the upper triangle of $\mathbf{R}_p$. Iterating over each element of the triangle is referred to as a sweep and several sweeps are required in order to achieve convergence.
A straight forward implementation of this algorithm based on IEEE 754 single precision floating point arithmetic has been evaluated in terms of computational performance requirements on an embedded field programmable gate array (FPGA) receiver. An Altera NIOS II/f processor was used as central processing unit (CPU) including a single precision floating point unit (FPU). However, decomposition of a 4×4 matrix in single precision floating point unit could not be achieved in real-time assuming a projector update rate at 1 kHz (approx. 2.7 ms are required at a clock rate of 100 MHz).
Thus, a fixed point implementation has been worked out. In following section containing the numerical results of this paper it is shown that 16-bit operands for eigenvectors and -values provide sufficient accuracy for interference mitigation at pre-correlation stage. In addition, a coordinate rotation digital computer (CORDIC) approximation [13] has been used for computing the elements of the rotation matrices $\mathbf{G}_p$. This approximation was chosen since it is possible to interleave computation of the arctan, sine, and cosine functions in a single loop. Regarding the complex rotation angle α, a coarse approximation has been implemented where α can only be assumed 0 or $\pi/2$.
Considering these aspects, it can be shown that the eigendecomposition can be executed on the same platform in less than 200 μs which leaves sufficient performance for the remaining tasks (i.e. signal acquisition, tracking, message decoding, etc.). The FPU is not required for the fixed point implementation anymore.

Power iteration

At post-correlation stage, only the eigenvector referring to the dominant eigenvalue of $\mathbf{R_{yy}}$ is required. A very simple but efficient algorithm for this case is the so-called power iteration which is briefly summarized in Alg.2. An ap-

Algorithm 2 Power iteration

1: $\mathbf{u}_0 = \frac{1}{\sqrt{M}} \cdot [1, 1, ..., 1]^T$
2: **for** $q = 0 \rightarrow Q - 1$ **do**
3: $\quad \mathbf{x} = \mathbf{R_{yy}} \cdot \mathbf{u}_q$
4: $\quad \lambda_q = \mathbf{u}_q^H \cdot \mathbf{x}$
5: $\quad \mathbf{u}_{q+1} = \frac{\mathbf{x}}{\|\mathbf{x}\|_2}$
6: **end for**
7: $\mathbf{u}_d = \mathbf{u}_Q$

proximation of the eigenvector referring to the maximum eigenvalue is achieved by successive multiplication of the covariance matrix by an estimate $\mathbf{u}_q$.
In case of the beamforming at post-correlation stage, iterations can be spread over time (i.e. only one iteration is computed with each covariance matrix update, assuming slowly changing matrices). Instead of initializing $\mathbf{u}_0$ as shown in Alg.2, $\mathbf{w}_{opt}$ of the previous update is used. This selection of $\mathbf{u}_0$ has two advantages: First, the computational requirements are clearly reduced (since convergence is achieved in one iteration) and second, the carrier phase at the discriminator input remains stable.
The normalization (line 5) is a critical step regarding the efficient implementation on embedded platforms. Instead of using the straight forward approach (i.e. computing the root of summed squares) an alternate algorithm [14] has been implemented. Concerning the costs for the beamforming at post-correlation stage, the following estimates have been measured on the embedded receiver: $T_{acc} \approx 5\ \mu$s are required for the accumulation of the actual correlator output to the covariance matrix and $T_{it} \approx 26\ \mu$s for computing one iteration of Alg.2. The overall load T_L for the beamforming at post-correlation stage can be approximated as follows:

$$T_L \approx N_{sv} \cdot (\frac{T_{\mathbf{y}}}{T_p} \cdot T_{acc} + T_{it}), \tag{58}$$

where N_{sv} denotes the number of space vehicles in view and T_p is the correlator predetection time.

NUMERICAL RESULTS

In this section we will analyze the performance of the two-step blind adaptive beamforming. First, a complex and exhaustive simulation scenario allowing a comprehensive analysis of the major effects a GNSS receiver installed on a car has to cope with will presented. Afterwards an analysis of the simulation results using a full resolution floating point unit implementation will be discussed and an improving operation for the evaluation of the post-correlation covariance matrix using forward-backward averaging [10] will be evaluated. Finally the results obtained in floating point resolution will be compared with a fixed point hardware implementation of the prewhitening module.

Scenario Description

In our simulation we consider a centrosymmetric uniform rectangular array (URA) consisting of 2×2 ($M = 4$) isotropic antenna elements equally spaced by $\lambda/2$, where λ is the wavelength of the carrier frequency of the signal. A simulation scenario was build up in order to cover some of the most important environment conditions in one run. The scenario considers a moving receiver, in this case a car, in different typical situations like driving a curve driving straight stretches or stop at a traffic light (Fig.1). During the track the receiver always was able to have a line-of-sight to the satellite signal, while it was affected by a bandlimited Gaussian interference (jammer) and four different multipath. For the scenario definition please refer to Table 1. In

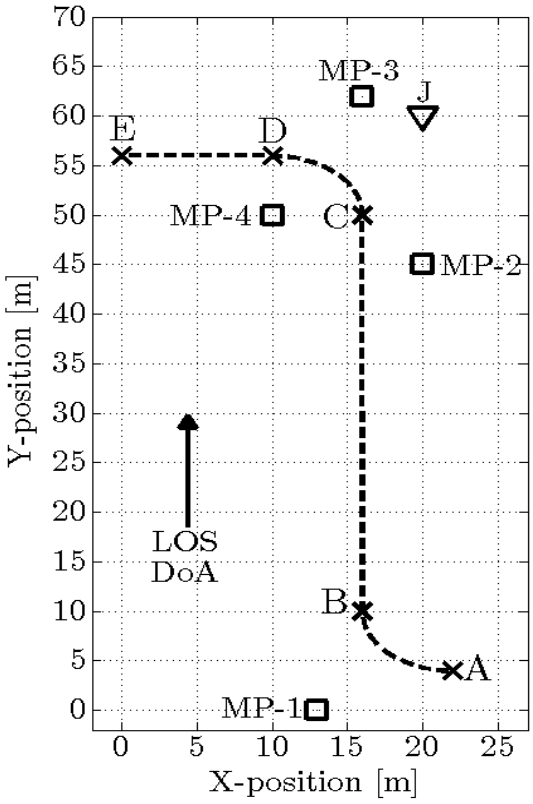

Fig. 1 Graphical description of simulation scenario

our case we considered scattering multipath signals having a gamma distributed amplitude and a uniform distributed phase. For all the signals the propagation time-delays, the Doppler shifts and the DoAs were considered based on the position and velocity of the receiver. Note that since the

TID	Track	Event description	Time [s]	Duration [s]	Velocity [km/h]
1	A	USER STOPS	0	5.0	0
2	A $\rightarrow$ B	USER MOVES	5.0	1.7	20
-	-	MP-1 ON	5.0	6.6	-
3	B	USER STOPS	6.7	2.0	0
-	-	MP-2 ON	7.0	4.6	-
4	B $\rightarrow$ C	USER MOVES	8.7	2.9	50
-	-	J ON	10.0	till end	-
5	C	USER STOPS	11.6	1	0
-	-	MP-3 ON	11.6	2.7	-
-	-	MP-4 ON	11.6	till end	-
6	C $\rightarrow$ D	USER MOVES	12.6	1.7	20
7	D $\rightarrow$ E	USER MOVES	14.3	0.7	30
-	E	END	15.0	-	-

Table 2 Simulation scenario detailed description

jammer occupies the whole receiver bandwidth the only effective counteracting action can be performed via a spatial filtering. The route covered by the car illustrated in Fig.1 is described in detail in Table 2. Observing the scenario it makes sense of splitting it in seven sub-scenarios, each indicated by a Track-ID number (TID). Each sub-scenario characterizes a particular combination of both user and environment conditions (e.g. during TID1 the user is static and neither RFI nor multipath is present).

Software Results

Fig.2 shows the array RFI attenuation at DoA of the jammer (DoA_J). The dependency on the observation time of the pre-correlation spatial covariance matrix ($T_{\mathbf{x}}$) is also shown indicated by different colors. The results were obtained using a projector update frequency of $\frac{1}{T} = 1\ KHz$, with the only exception for $T_{\mathbf{y}} = 5\ ms$ where the update frequency was set to $0.2\ KHz$. As it can be expected longer $T_{\mathbf{x}}$ exhibits better performance when the user position is static (TID5) and in general when the DoA_J is not varying significantly (TID4). On the other hand, when the user is moving (TID6 and TID7) a shorter observation time $T_{\mathbf{x}}$ should be preferred. If we consider a $T_{\mathbf{x}} = 0.5\ ms$ as a trade-off for the scenario under consideration the prewhitening would be able to attenuate a wideband interference of at least $47.5\ dB$. Fig.3 depicts the average array gain at the DoA of the LOS signal (DoA_{LOS}) during each TID. The post-correlation spatial covariance matrix observation time $T_{\mathbf{y}}$ was varied from $20\ ms$ to $200\ ms$. From the behavior of the array gain it can be observed that a shorter observation time has slightly better performance in case the user is moving fast (TID2, TID4, TID6 and TID7). On the contrary, the best performance obtained when the user is in a static position is of course those using a longer observation time $T_{\mathbf{y}}$. This becomes particularly evident for TID5 since for TID1 and TID3 the array

Scenario parameters	
A,B,C,D,E	Ref.Rx.postions (A=start)
Track length	approx. $69\ m$
Track duration	$15\ s$
LOS DoA	Satellite signal DoA
Type	GPS-L1 CA, PRN1
Bandwidth	$B = 4\ MHz$ (one-sided)
N_0	$-204\ dBW/Hz$
Power	$-157\ dBW$
C/N_0	$47.5\ dB - Hz$
DoA_{LOS} elevation	fixed at 60°
DoA_{LOS} azimuth	time varying
DoA_{LOS} max. variation	1° each $16.6\ ms$ (max)
$MP - x$	Multipath source ($x = 1..4$)
C/N_0	Gamma dist. with mean $[44.5, 42, 43, 42]\ dB - Hz$
Phase	Uniform distributed $[0, 2\pi]$
DoA_{MP_x} elevation	fixed at $[20^\circ, 15^\circ, 15^\circ, 22^\circ]$
DoA_{MP_x} azimuth	time varying
DoA_{MP_x} max. variation	1° each $10.0\ ms$
J	Jammer
Type	Bandlimited noise
Bandwidth	$B = 4\ MHz$ (one-sided)
Power	$-115\ dBW$
DoA_J elevation	fixed at 20°
DoA_J azimuth	time varying
DoA_J max. variation	1° each $10.0\ ms$

Table 1 Simulation scenario parameters

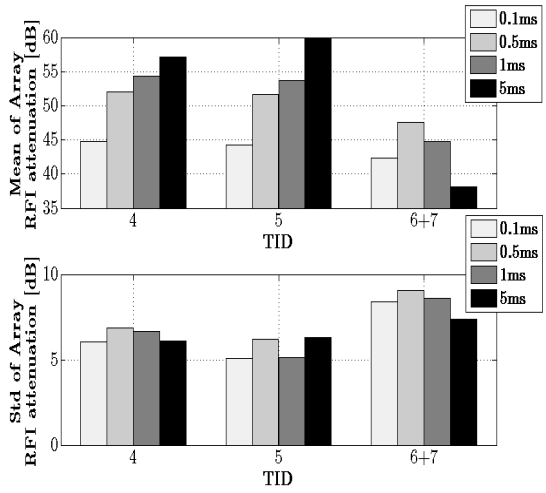

Fig. 2 Array RFI attenuation at DoA_J: a) mean and b) standard deviation

gain reaches the maximum value of $10 \cdot \log_{10}(M) \approx 6\,dB$ for different observation time. Fig.4 shows the ratio between the array gain at DoA_{LOS} and the array gain at the DoA of the four multipath (DoA_{MP_x}). The dependency of $T_{\mathbf{y}}$ on the respective array gain at DoA_{MP_x} is also a useful figure of merit in order to understand the impact the scattering echoes effectively have on the LOS signal tracking. No variations of the array gain can be associated to a marginal effect of the multipath on the tracking performance. Regarding the array gain at DoA_{MP_x} and the dependency on $T_{\mathbf{y}}$ as well as on DoA dynamics the same considerations are valid as discussed above for the array gain at DoA_{LOS}. The only incongruity consists in the fact that a longer integration time contributes at the same time to the decorrelation of the LOS signal from the multipath signals. In general, the longer $T_{\mathbf{y}}$ is chosen the higher the multipath decorrelation becomes. At the same time the eigenbeamformer can not optimally follow the dynamic of the LOS signal. As depicted in Fig.4 the resulting loss in array gain is compensated by higher multipath decorrelation and thus by a higher array LOS to multipath ratio.

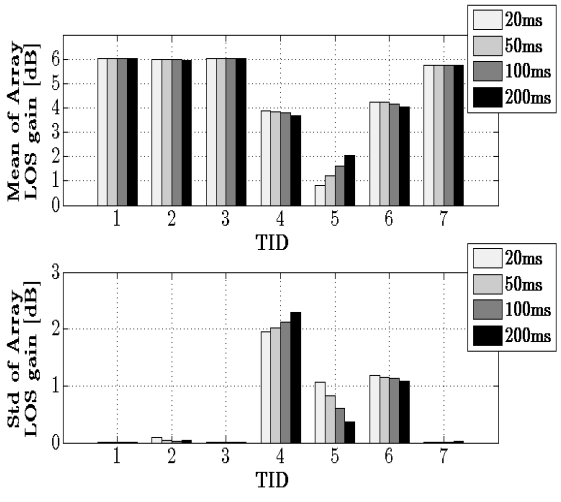

Fig. 3 Array gain at DoA_{LOS}: a) mean and b) standard deviation

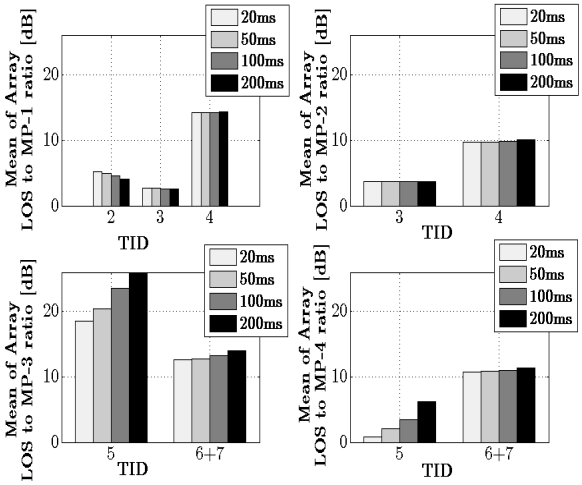

Fig. 4 Array $LOS\ to\ MP_x$ ratio

Forward-Backward Averaging

In order to obtain a better resolution for the eigenvector related to the LOS signal under tracking as well as to decorrelate the undesired scattering signals without having to increase the $T_{\mathbf{y}}$, we apply forward-backward averaging (FB) [10]:

$$\hat{\mathbf{R}}_{\mathbf{fb}} = \frac{1}{2}\left(\hat{\mathbf{R}}_{\mathbf{yy}} + \mathbf{J}\,\hat{\mathbf{R}}^{*}_{\mathbf{yy}}\,\mathbf{J}\right) \tag{59}$$

where

$$\mathbf{J} = \begin{bmatrix} \mathbf{0} & \cdots & \mathbf{1} \\ \vdots & \iddots & \vdots \\ \mathbf{1} & \cdots & \mathbf{0} \end{bmatrix} \in \mathbb{R}^{M \times M} \tag{60}$$

is the exchange matrix.
Fig.5 shows the benefit of using FB, the results were obtained with a $T_{\mathbf{y}} = 100\ ms$.

Fixed point vs. Floating point implementation

The eigendecomposition required for the prewhitening by the two-step adaptive spatial filtering has been implemented on a FPGA hardware. While the software based receiver makes use of double precision floating point unit (64-bit) data, the FPGA hardware was based on 16-bit fixed point unit data operands. Both software and hardware simulations received the same input data (14-bit). We focus only on the FPGA implementation of the prewhitening since the low data rate at which the post-correlation beamforming operates, allows the algorithm to be implemented on a floating point processor. Note that the prewhitening

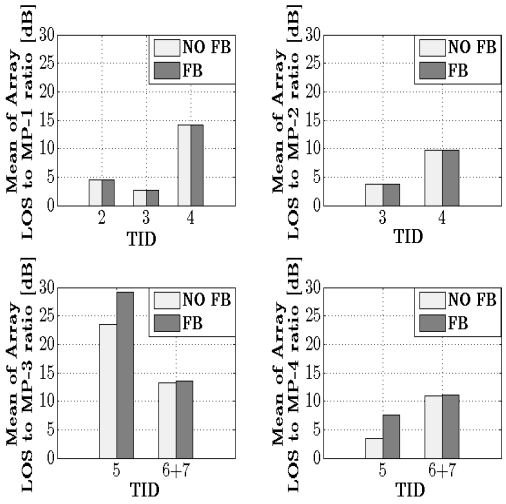

Fig. 5 Array $LOS\ to\ MP_x$ ratio using Forward-backward averaging

is fully independent from the tracking loops and from the post-correlation beamformer. Consequently any dissimilarity between hardware and software results are only due to the resolution loss.

The input data resolution was set to 14-bit while the resolution of the output data after applying the projector was 12-bit, the projector itself has a resolution of 16-bit. In Fig.6 the array attenuation at DoA_J for both the floating point and fixed point implementation using a projector update interval of 1ms and $T_{\mathbf{x}} = 0.5\ ms$ is depicted. In the worst case the hardware implementation achieves a lower jammer suppression capability of about 7 dB in comparison with the floating point approach. Nevertheless the hardware implementation is able to reduce the jammer impact of more than $40\ dB$.

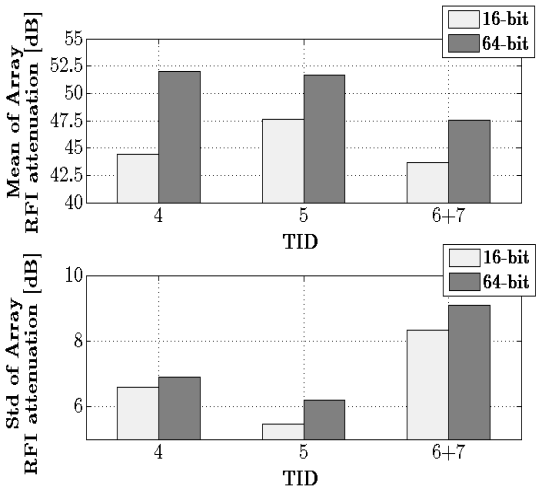

Fig. 6 Array attenuation at DoA_J using fixed point resolution: a) mean and b) standard deviation

CONCLUSION

In this work we have proposed a two-step blind adaptive beamforming approach based on orthogonal projections at pre-correlation and post-correlation stage for GNSS, for which knowledge of the array response and a spatial reference for the LOS signal are not required. A cost-analysis in terms of processing cycles on an embedded processor for the covariance matrix computation and eigendecomposition was presented.

A software bit accurate representation of the GNSS receiver hardware platform was used for performance evaluation. Simulation results have shown that the proposed blind adaptive beamforming approach based on orthogonal projections is capable of effectively mitigating interference and multipath signals. The presented approach provides a well balanced trade-off between computational complexity and performance.

REFERENCES

[1] M. D. Zoltowski and A. S. Gecan, "Advanced adaptive null steering concepts for GPS," in *Military Communications Conference, 1995, MILCOM '95*, San Diego, CA, USA, November 1995.

[2] G. Seco-Granados, J. A. Fernández-Rubio, and C. Fernández-Prades, "ML Estimator and Hybrid Beamformer for Multipath and Interference Mitigation in GNSS Receivers," *IEEE Transactions on Signal Processing*, vol. 53, no. 3, March 2005.

[3] S. Daneshmand, A. Broumandan, and G. Lachapelle, "GNSS Interference and Multipath Suppression Using an Antenna Array," in *Proceedings of ION GNSS 2011*, Portland, OR, USA, September 2011.

[4] C. Fernándes-Prades, P. Closas, and J. Arribas, "Eigenbeamforming for Interference Mitigation in GNSS Receivers," in *Proceedings of International Conference on Localization and GNSS, ICL-GNSS 2011*, Tampere, Finnland, June 2011.

[5] M. V. T. Heckler, M. Cuntz, A. Konovaltsev, L. A. Greda, A. Dreher, and M. Meurer, "Development of Robust Safety-of-Life Navigation Receivers," *IEEE Transactions on Microwave Theory and Techniques*, vol. 59, no. 4, pp. 998 – 1005, April 2011.

[6] M. Viberg and A. L. Swindlehurst, "Analysis of the Combined Effects of Finite Samples and Model Errors on Array Processing Performance," *IEEE Transactions on Signal Processing*, vol. 42, no. 12, December 1994.

[7] K. Pensel, H. Aroudaki, and J. A. Nossek, "Calibration of Smart Antennas in a GSM Network," in *Proceedings of Signal Processing Advances in Wireless Communications (SPAWC)*, Annapolis MD, U.S.A., May 1999.

[8] A. Konovaltsev, N. Basta, L. A. Greda, M. Cuntz, M. V. T. Heckler, and A. Dreher, "Calibration of Adaptive Antennas in Satellite Navigation Receivers," in *Proceedings of the Fourth European Conference on Antennas and Propagation (EuCAP), 2010*, Barcelona, Spain, April 2010.

[9] J. Li and P. Stoica, Eds., *Robust Adaptive Beamforming*. John Willey & Sons, Inc., 2006.

[10] S. Pillai and B. H. Kwon, "Forward/backward Spatial Smoothing Techniques for Coherent Signal Identification ," *IEEE Transactions on Acoustics, Speech and Signal Processing*, vol. 37, pp. 8–9, January 1989.

[11] T. J. Shan, M. Wax, and T. Kailath, "Spatial Smoothing Approach for Location Estimation of Coherent Sources ," *IEEE Transactions on Acoustics, Speech and Signal Processing*, vol. 33, pp. 806–811, August 1985.

[12] W. H. Press, S. A. Teukolsky, W. T. Vetterling, and B. P. Flannery, *Numerical Recipes 3rd Edition: The Art of Scientific Computing*. Cambridge University Press, 2007.

[13] R. Andraka, "A survey of CORDIC algorithms for FPGAs," in *Proceedings of the 1998 ACM/SIGDA sixth international symposium on Field programmable gate arrays*, Monterey, CA, USA, February 1998.

[14] C. Seol and K. Cheun, "A Low Complexity Euclidean Norm Approximation," *IEEE Transactions on Signal Processing*, vol. 56, no. 4, pp. 1721 –1726, April 2008.